

Vol. 9, N°1 (2025) 166 - 184

Hydro-climatic variability and change in the Ferlo catchment (Senegal)

Assane Ndiaye¹, Ibrahima Camara², Mamadou Lamine Mbaye^{1,*}

¹Laboratoire d'Océanographie, des Sciences de l'Environnement et du Climat (LOSEC), Université Assane SECK de Ziguinchor, BP 523, Sénégal

²Laboratoire de Physique de l'Atmosphère et de l'Océan-Siméon Fongang (LPAOSF)/ESP/UCAD

Received: 26 April 2025 / Received in revised form: 15 June 2025 / Accepted: 26 June 2025

Abstract:

In Senegal, climate change raises concerns about the availability of reliable climate information to guide policymakers in developing effective adaptation strategies and reducing population vulnerability. To address this, we examined hydro-climatic variability and change in the Ferlo catchment, a region of socio-economic importance. Using observational data from the Climatic Research Unit (CRU) and outputs from regional climate models (REMO, CCLM4-8-17, and RCA4) under RCP4.5 and RCP8.5 scenarios, we assessed future climate trends. The results indicate a significant decrease in average and cumulative rainfall, marked by lower isohyets and a southward shift across the basin. The rainy season is projected to shorten between 2006 and 2100, lasting around 85 days in the north, 90 in the center, and 98 in the south compared to 89, 94, and 103 days respectively during 1976–2005. Additionally, a reduction in mean daily rainfall intensity from north to south is projected. These changes highlight the urgent need for adaptation. Policymakers must revise agricultural calendars, improve water resource management, and adapt livestock practices. Furthermore, implementing social safety nets and early warning systems will be essential to protect vulnerable communities from increased climate-related risks and ensure resilience in the face of growing climatic challenges.

Keywords: Hydro-climatic indices, climate change, Variability, Ferlo Catchment.

1 Introduction

The vital role of water for life on earth and for activities in general makes scientists and managers now concerned about the consequences of climatic hazards on the hydrological cycle, availability, and quality of groundwater and surface water [1]. It is considered to be one of the most serious threats to sustainable development, with

Email address: mlmbaye@univ-zig.sn (M.L. Mbaye) https://doi.org/10.70974/mat09125166



^{*} Corresponding author:

expected adverse effects on human health, food security, economic activity, water, and other natural resources. While the global climate has natural variations, according to the fifth IPCC report, most of the observed rise in global mean temperature since the middle of the 20th century is most likely due to the greenhouse (GHGs) gas concentrations [2]. The climate variability impacts vary from one region of the globe to another, with particularly important socio-economic consequences in developing countries [3].

Africa is the most vulnerable continent due to its high exposure and low adaptive capacity [4]. Several impact studies over West Africa have shown that water resources are significantly impacted by climate change ([5], [6]). For much of Africa, knowledge about recent climate change is limited, due to weak climate monitoring and gaps in coverage that continue to exist [2]. According to [7], West Africa is among the most affected areas, where the key development sectors of Sahelian countries, notably the environment, agriculture, and water resources, are considered highly vulnerable to climate change. The latter will be accompanied by new rainfall and stream flow regimes. [8] reported irregularities in the rainy season, an increase of extreme rainfall and temperatures over the region; this is threatening food security.

In Senegal, it presents serious risks for agriculture, which is mainly rain-fed, water resources, and coastal areas. These three sectors occupy an important place in the national economy and their sensitivity to the climate impact is considered in the Emerging Senegal Plan [9]. Given the vulnerability of these resources, the

evolution of water resources is becoming a worrying issue for many localities in Senegal, particularly the Ferlo zone, where agriculture, breeding, and forestry are the main activities of the populations. In this context, our study aims to analyze the hydroclimatic conditions and to establish indicators of climate change in the Ferlo catchment.

The paper is structured as follows: the data and methods are described in Section 2. The results and discussions are presented in Section 3, and the conclusion is given in Section 4.

2 Material and methods

2.1 Study Area of the watershed of Ferlo

The study is focused on the Ferlo catchment located in Senegal (West Africa). It is bounded by the Senegal River Valley to the north and the groundnut basin to the south. The Ferlo catchment area (Figure 1) lies between latitudes 16°15 and 14°30 North and longitudes 12°50 and 16° West. It covers an area of about 70,000 km². It is the largest eco-geographic region in Senegal, with the highest number of pastoralists of any other region in the country. Extensive livestock farming in this area uses natural pastures [10] and operates in two distinct modes. During the rainy season, the pasture is essentially made up of the herbaceous stratum, while during the dry season, the woody stratum contributes very strongly to the livestock's diet.

Ferlo is located in the Sahelian domain characterized by the alternation of two seasons: a dry season that lasts 9 months (October to June) and a rainy season of 3 months. Rainfall remains low and very unstable with an average of 422.6 mm/year for a coefficient of variation of 0.3 over the period 1951-2004 [11] . The temperature generally varies between a minimum of 18°C which can exceed 40°C in May.

2.2 Material

Three types of data were used in this study: (1) daily rainfall data from four stations (Sagata, Richard-Toll, Barkedji, and Linguère) available for the period 1981-1990 and obtained from Senegal's National Meteorological Agency (Figure 1); (2) monthly gridded data of rainfall and temperature from the Climatic Research Unit (CRU). These data have a horizontal

(spatial or horizontal) resolution of 0.5° x 0.5° (e.g., 50 km x 50 km) for the period 1901 to 2013; (3) daily data from a set of simulations (historical scenarios) from the Coordinated Regional Climate Downscaling Experiment [12] over Africa on a 0.44° grid. They cover the 1950-2100 period under the representative concentration pathway scenarios (RCP4.5 and RCP8.5). For this study, we used four regional models (Table 1), each of which climate included four variables (precipitation, mean surface temperature, maximum, and minimum temperature). In addition to these variables, one of the models (REMO) contains other variables, such as total runoff and surface runoff. These models have already been used successfully in Africa [13-17].

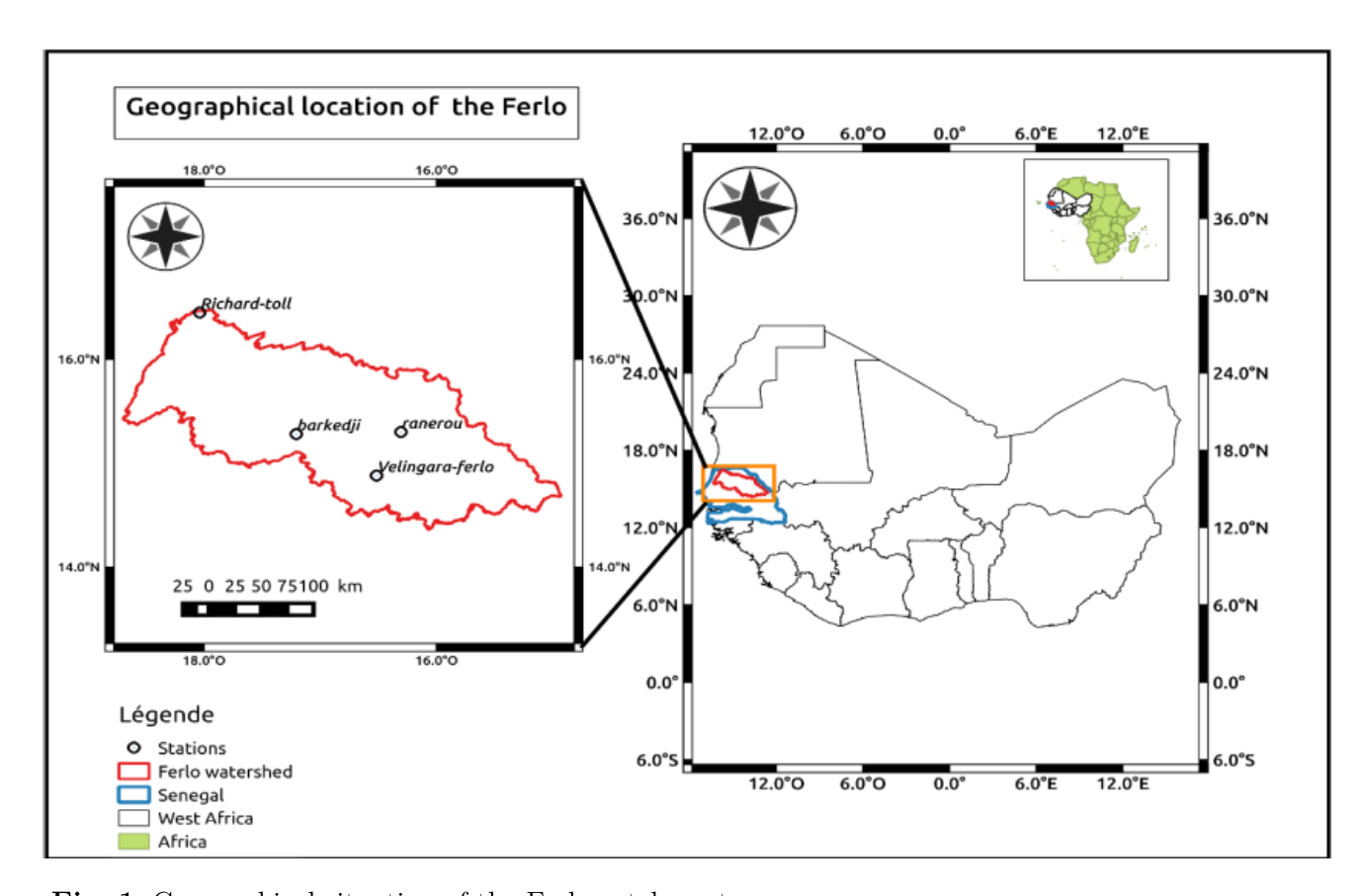


Fig. 1. Geographical situation of the Ferlo catchment.

Table 1
Characteristics of the climate models used.

RCM Models	Driving GCM	Institution	Variables	Experiment
REMO	MPI-M-MPI-ESM	MPI-CSC	Pr; mrro,mrros	historical
				rcp4.5
				rep8.5
CCLM4-8-17	ICHEC-EC-	CLMCom	\Pr	historical
	EARTH			rcp4.5
				rcp8.5
RCA	MIROC-MIROC5	SMHI	Pr	historical
				rcp4.5
				rcp8.5
CClM4-8-17	MPI-M-MPI-ESM	MPI-CSC	\Pr	historical
				rcp4.5
				rcp8.5

2.3 Methods

The analyses are mainly focused on some hydrological parameters and climate indices. For the former, we compute the runoff coefficient; its equation is given by the following:

$$C_r = \frac{R_s}{P_r} \tag{1}$$

Where R_s is Blade water run-off and Pr is total precipitation considered during the rainy season (JJASO). To determine the contribution of each runoff component to the total runoff, we calculated the ratio of each component (surface and base flow) to the total runoff.

$$r_{st} = \frac{R_s}{R_t} \tag{2}$$

$$r_{bt} = \frac{R_b}{R_t} \tag{3}$$

Where R_b is the base runoff and R_t is the total runoff. Furthermore, we have also estimated the mean rainfall intensity and frequency, the rainy season onset (start), cessation (end) and length. The rainy season onset (RSO) is defined as the first

date after May 1st when at least 15 mm of rainfall occurs over a period of 3 consecutive days, with no dry spell longer than 10 days within the following 30 days [18] (sentence to be reformulated, not clear). The rainy season cessation (denoted RSC) is defined as the date after September 1st on which a minimum of 20 consecutive days without rainy days (rainfall less than 1mm). The rainy length (denoted RSL) is obtained by the subtraction between the end and beginning dates of the season (RSL = RSC -RSO).

To evaluate the change of hydro indices in the future, we have considered two horizons under two scenarios RCP4.5 and RCP8.5 described by [19]: the near future, which expands from 2021 to 2050, and the far future from 2071 to 2100; the reference period expands from 1976 to 2005. This study was used to characterize future changes compared to the baseline (1971-2005).

The future changes of each hydro climate index (I) are estimated as :

$$I = 100. \frac{FL - HIST}{HIST} \tag{4}$$

Where FL represents the average over the near and far future (2021-2050, 2071-2100) and HIST is the mean value of the hydro climate index over the period (1976-2005).

3 Results

3.1 Climatic indices

3.1.1 Variation of isohyets in the past (1976 to 2005) and in the future (2021 to 2051 and 2071 to 2100)

With regard to spatial variation in the future, our studies reveal for the periods 2021-2050 and 2071-2100 under the scenarios (rcp4.5 and rcp8.5) a spatial variation of isohyets towards the south. For the near future (Figure 2, left), a much greater shift from the reference period is observed under the RCP8.5 scenario than under the RCP4.5 scenario. This period is marked by the disappearance of the 600 mm isohyet and the presence of the 200 mm isohyet towards the north of the basin. This confirms the decrease in rainfall in the future.

For the distant future, a migration of the 300 mm isohyet towards the center of the basin and the presence of the 500 mm isohyet in the south of the basin are observed (Figure 2, right). These low-value

isohyet shifts will symbolize a significant decrease in precipitation in this area.

Therefore, as one moves southward in the area, rainfall increases, which is confirmed by the work of [20], who mentions a migration of 400 and 500 mm values toward the south in the 1970s.

3.1.2 Evolution of precipitation intensity and accumulation in the future

Figure 3 shows the spatial change in daily rainfall intensity obtained from the ensemble average of the four climate models. The latter (Figure 2) shows an irregular variation with lower intensities in the North than in the South. Furthermore, the evolution of the intensity in the future varies irregularly according to the periods (near future, far future), and scenarios (RCP4.5, RCP8.5). In the near future, both scenarios show respectively a decrease (up to -8%) in the relative gap in the North and the Central Eastern part, but also an increase of 2 to 10% for the rest of the Basin. In the distant future, the decrease in the relative gap will be observed in almost all parts of the basin, but much more intensely in the North (-8 and -10%) with RCP8.5.

The results are consistent with those of [21] and [22] in Senegal, who demonstrated a decrease in rainfall under the RCP8.5 scenario.

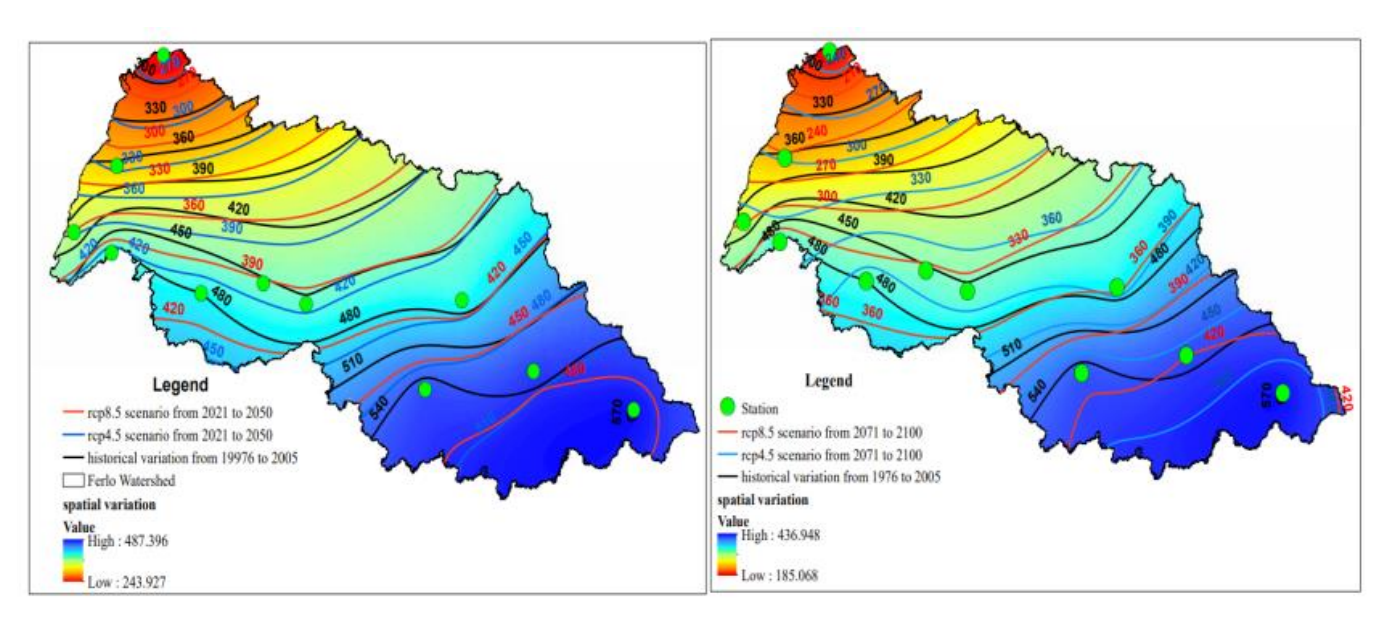


Fig. 2. Mean Isohyet, of the multi-model mean (MMM), for the historical period (black line), rcp4.5 (blue line), and rcp8.5 (red line): (left) for the near future (2012-2050) and (right) for the far future (2017-2100).

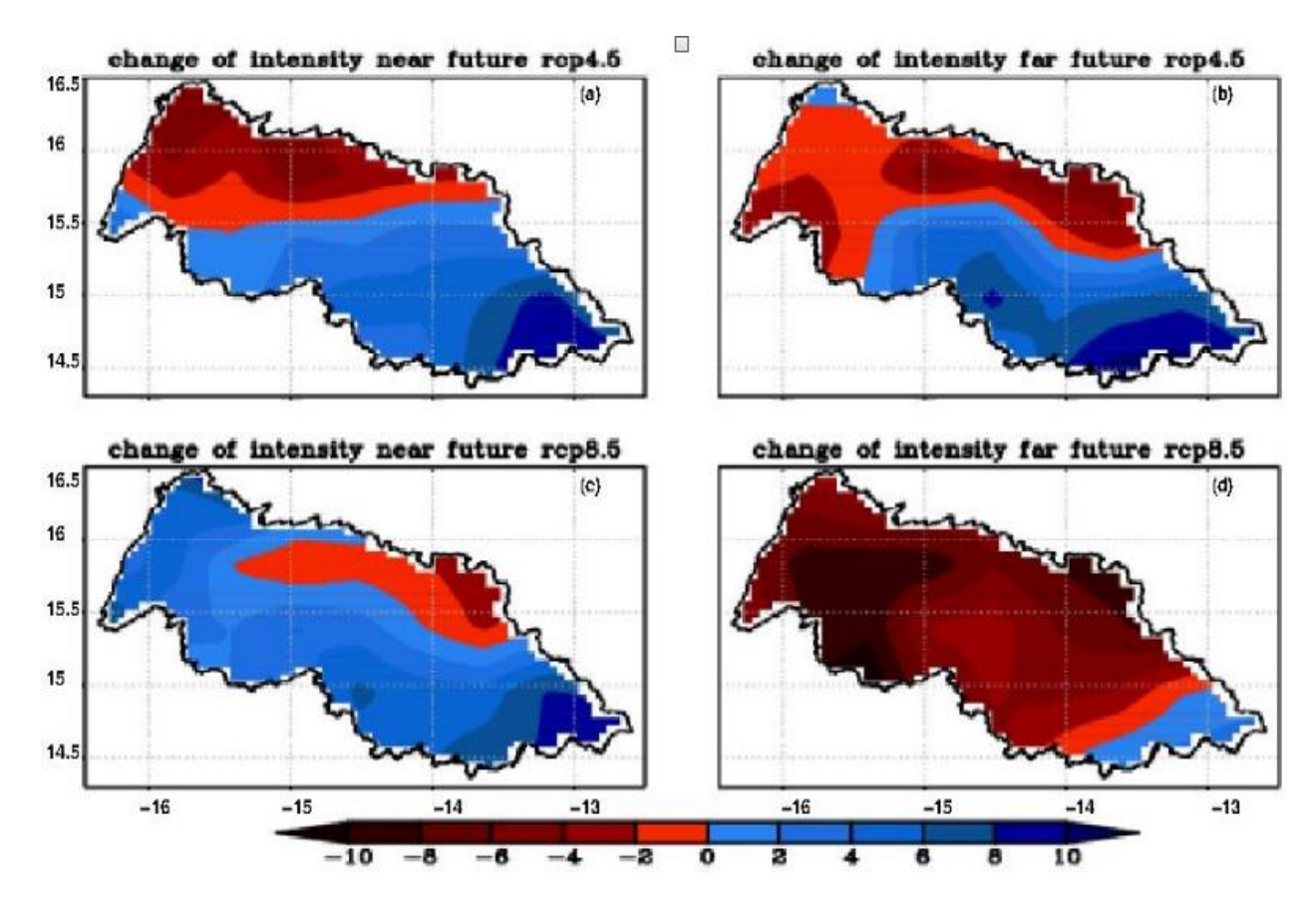


Fig. 3. Relative Changes (in %) of seasonal precipitation intensity obtained from the multi-model mean (MMM): (a) and (b) are changes under RCP4.5 for the near and far future, respectively. (c) and (d) are changes under RCP8.5 for the near and far future, respectively.

For cumulative daily rainfall (Figure 4), the overall average of the models predicts a decrease in the future that is unevenly distributed in space and time over the whole Ferlo area. In the near future, the RCP 4.5 and RCP8.5 scenarios show a much greater decrease in cumulative rainfall in the south than in the north, with values ranging between -6 and 3% respectively in these areas. In the distant future, the RCP4.5 scenario predicts a decrease of -3% almost homogeneous over the entire extent of the Basin; the RCP8.5 scenario observes a significant decrease that can go as far as - 45% in the North, from -27 to -39% in the center, and -15 to -24% in the south of the Basin. The results are in line with those of some previous studies. For example, [23] found a decrease of around 12.6 % by 2100 in the western Sahel. In Senegal, some studies also show this decrease in rainfall [21, 22, 24] under RCP8.5. [21] found a strong decrease in rainfall by 2080-2099 under the RCP8.5 scenario in Senegal. What about RCP4.5 [25] highlighted that the reduction in average rainfall in this region of West Africa could be partly caused by a weakening of moisture from local sources, which slows the hydrological cycle.

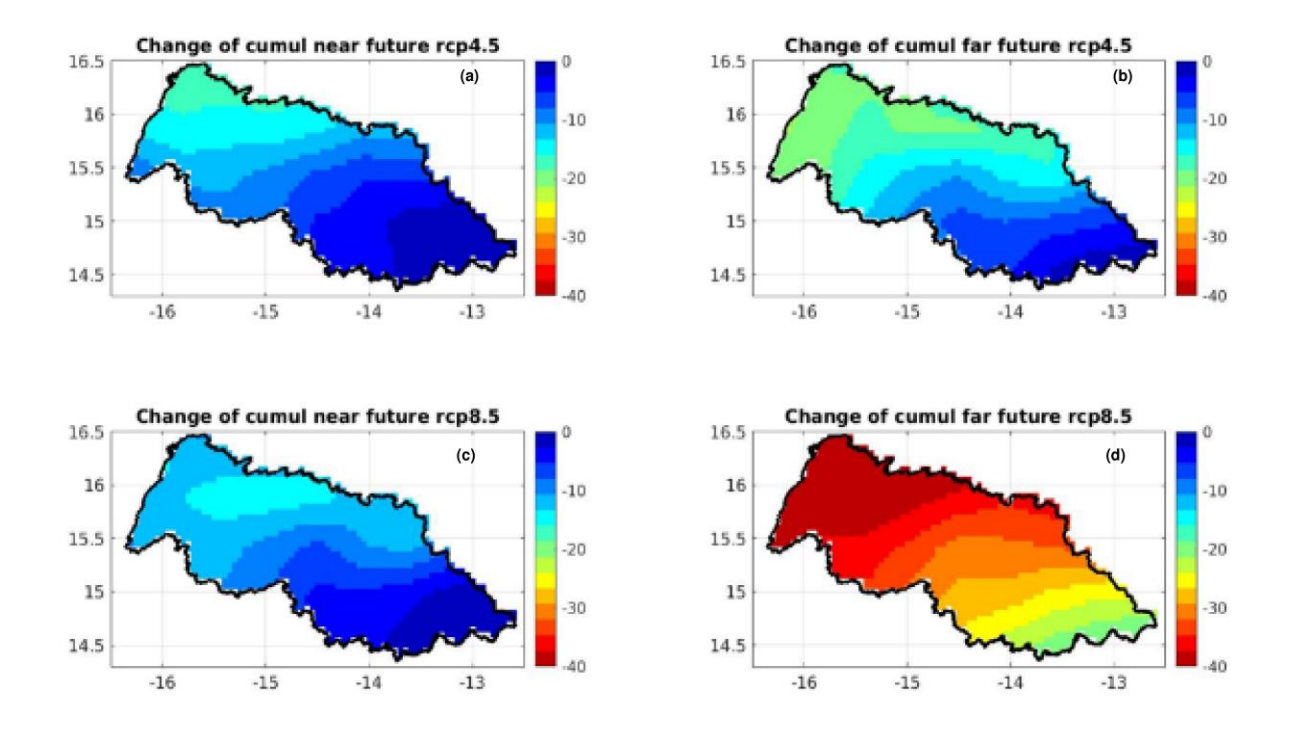


Figure 4: Relative Changes (in %) of cumulus obtained from the multi-model mean (MMM): (a) and (b) are changes under RCP4.5 for the near and far future, respectively. (c) and (d) are changes under RCP8.5 for the near and far future, respectively.

3.1.3 Rainy season length variation in the future

Figure 5 shows the spatial variation of the rainy season. This variation is irregular in time (near and far future) according to the RCP4.5 and RCP8.5 scenarios. The general average of the models shows a decrease in the rainy season. This decrease will be much more important in the extreme northern areas than in the south. In the coming years, the RCP4.5 scenario predicts a decrease of up to -10 to -15% in the north and -5% in the south. However, within the RCP8.5 scenario, the models predict a +5% increase in season length in the south-east of the basin.

In the far future (2071-2100), the decrease is almost homogeneous from the northwest to the southeast. The RCP8.5 scenario predicts a decrease of -20 to -25% in the northwest and -5 to -15% in the central and southwestern parts of the catchment area, respectively. This variation in the onset and offset of the rainy season contributes to the observed changes in its duration over time and space.

These results are in line with the studies of [26], who said that the beginning (onset) and end (cessation) of the rainy season in Senegal display a dual gradient: one oriented from southeast to northwest for the onset of the season, and another from south to north for the end of the season.

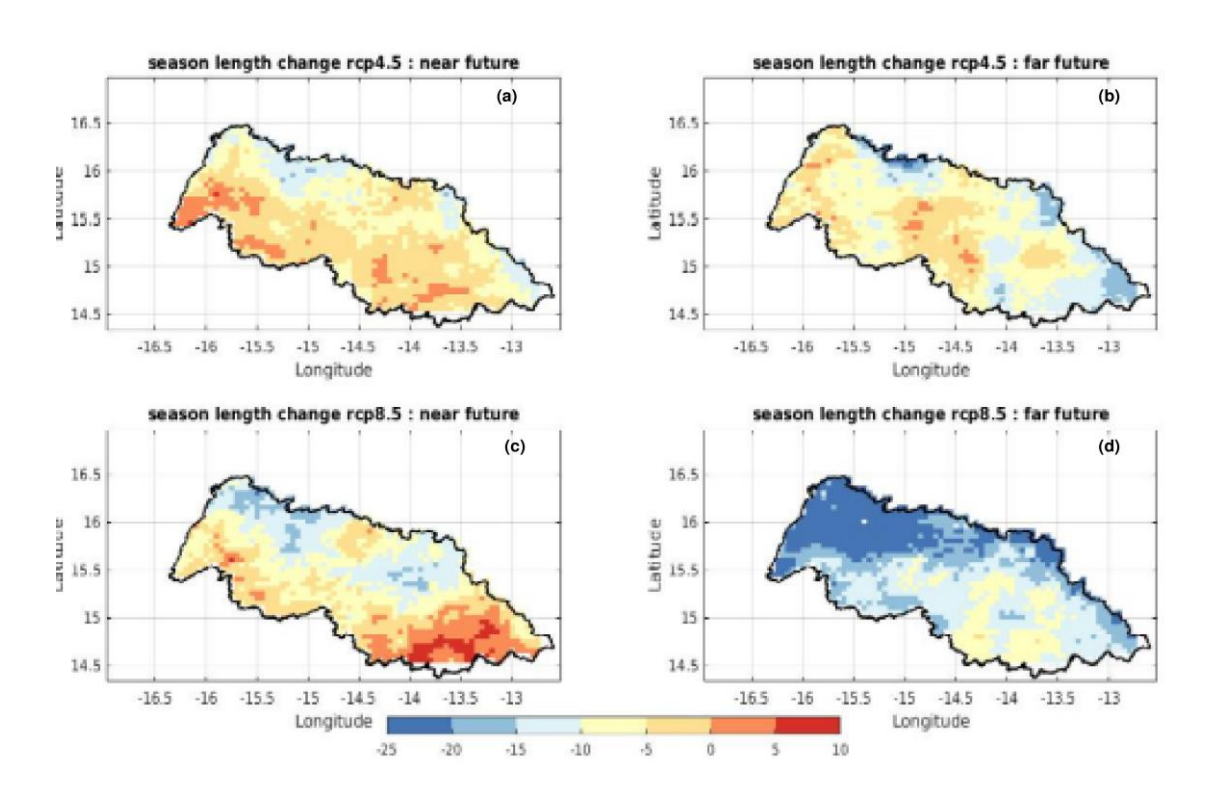


Figure 5: Relative Changes (in %) of the length of the rainfall period obtained from the multi-model mean (MMM): (a) and (b) are changes under RCP4.5 for the near and far future, respectively. (c) and (d) are changes under RCP8.5 for the near and far future, respectively.

3.2 Hydrological indices

3.2.1 Change in runoff coefficient

The spatial variation of the runoff coefficient in the Ferlo catchment is presented in Figure 6. The following results are calculated using the REMO2009 model. The variation is homogeneous in the future under the different scenarios RCP4.5 and RCP8.5, with positive values in the north and negative values in the center and south of the basin.

In the future (near and far) under the RCP4.5 scenario and in the near future under the RCP8.5 scenario, the value recorded in the North is between +10 and +120%.

In the center and south of the area, the runoff coefficient will be negative and varies between -10 to -100%.

However, in the distant future, with the RCP8.5 scenario, the runoff coefficient will decrease in the North until it reaches values between +10 and +30%.

This trend observed in the North could be due either to the vegetation cover, the soil types, or the location of the station, such as the Richard-toll station located in Senegal. The spatial distribution of vegetation cover in the Ferlo region, as illustrated in figure 7, reveals a significant spatial heterogeneity in NDVI values during the 2023 rainy season (June to August). Higher NDVI values are concentrated in the southern and eastern parts of the basin, indicating denser vegetation, while lower NDVI values dominate the northern zone, reflecting more arid or sparsely vegetated conditions. This vegetation pattern supports the spatial variation of the runoff coefficient presented in Figure 6, derived from the

REMO2009 model under RCP4.5 and RCP8.5 scenarios. The projected increase in runoff coefficient in the northern region, with values ranging from +10% to +120%in the near future, aligns with the lower NDVI values observed, suggesting limited vegetation cover and thus greater surface Conversely, the central southern zones exhibit negative runoff values (-10% to -100%). coefficient consistent with the denser vegetation detected by higher NDVI values, which likely promote increased infiltration and reduced runoff. In the distant future under RCP8.5, the projected decline in runoff in the north (to +10-30%) may be partially influenced by gradual vegetation recovery, though $_{
m this}$ remains limited. observations underscore the potential influence of vegetation cover on hydrological dynamics, particularly explaining localized trends near stations such as Richard-Toll in northern Senegal. Figure 8 illustrates the spatial distribution of surface soil moisture in the Ferlo catchment during the period from June to August 2023. A clear heterogeneity is observed, with a gradual increase in soil moisture from the northwest to the southeast of the basin. The lowest values (around $0.07 \text{ m}^3/\text{m}^3$) are found in the north while and central-western areas, southern and southeastern zones show higher soil moisture levels, reaching up to 0.17 m³/m³. This spatial pattern likely reflects the influence of rainfall gradients, soil types, and denser vegetation cover in the southern parts of the basin, as already highlighted in figure 7 (NDVI). These results support the variations in the runoff coefficient described in figure 6. Indeed, the low soil moisture observed in the north could explain the positive runoff coefficient

values in that region, as drier soils are less capable of water infiltration, thereby favoring runoff. Conversely, the more humid and vegetated southern zones show greater infiltration capacity, reducing surface runoff and explaining the negative values of the runoff coefficient. Therefore, the joint analysis of figures 6, 7, and 8 highlights the interdependence between vegetation cover, soil moisture, and runoff dynamics, underlining the impact of local physical conditions on the future evolution of the hydrological response of the Ferlo basin.

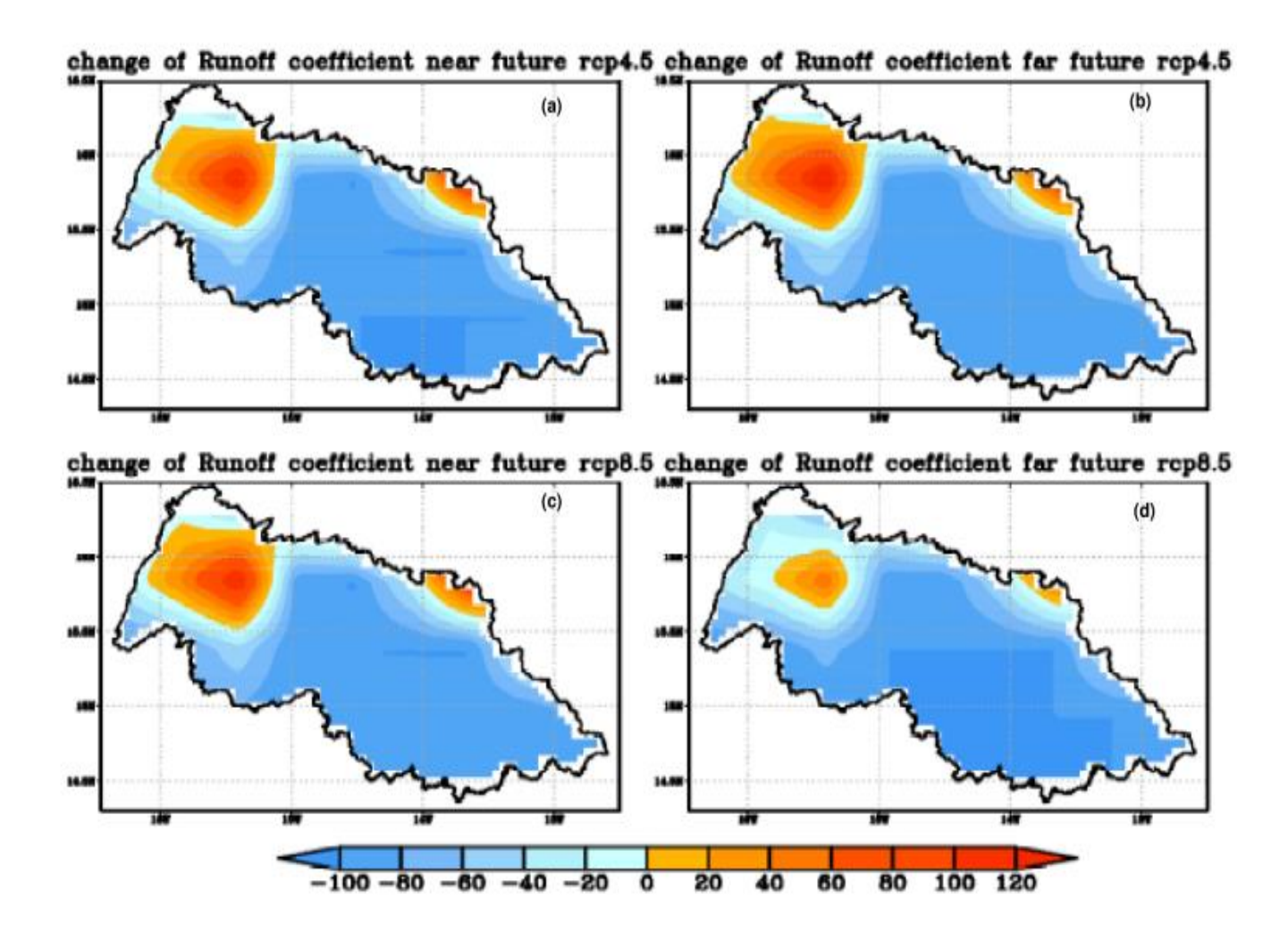


Fig. 6. Relative Changes (in %) of the runoff coefficient obtained from the model REMO2009: (a) and (b) are changes under RCP4.5 for the near and far future, respectively. (c) and (d) are changes under RCP8.5 for the near and far future, respectively.

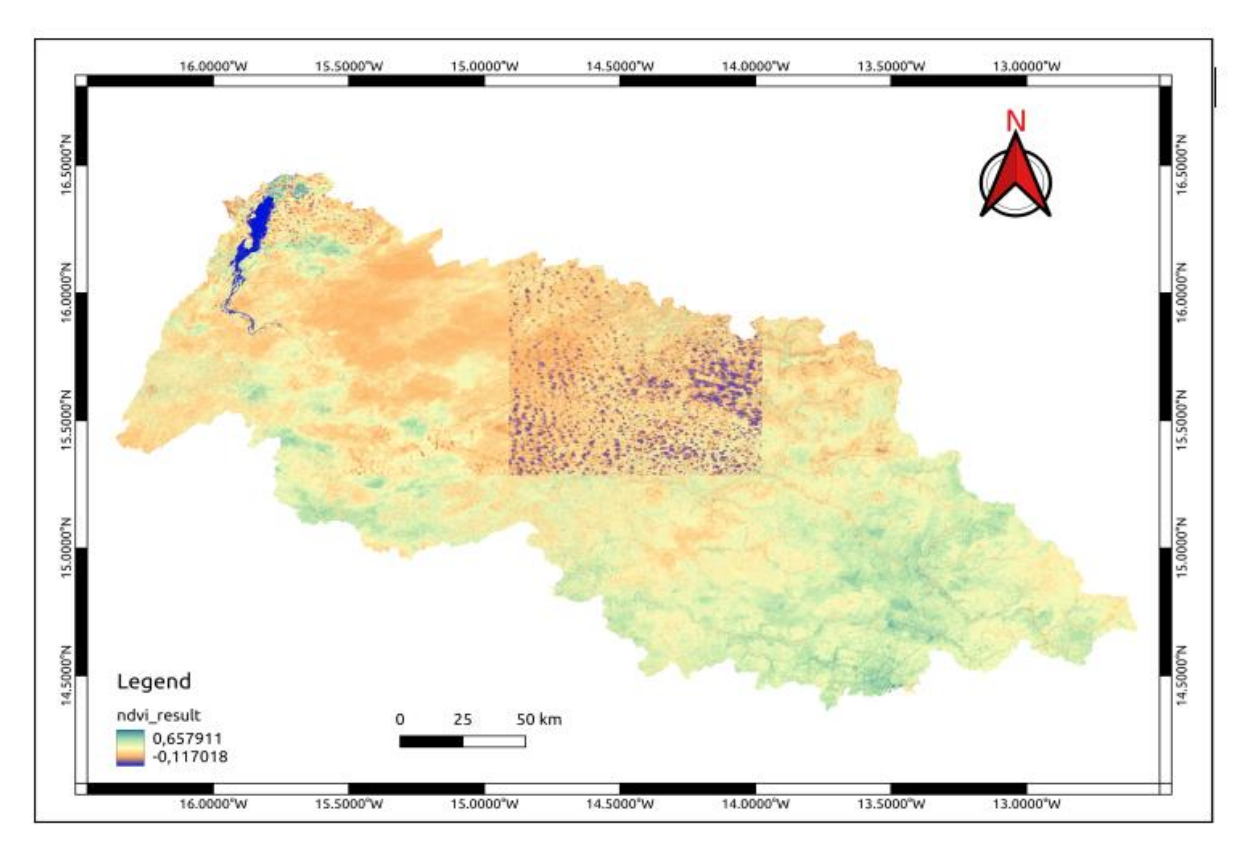


Fig. 7. NDVI Map of the Ferlo Region (Senegal) – June to August 2023.

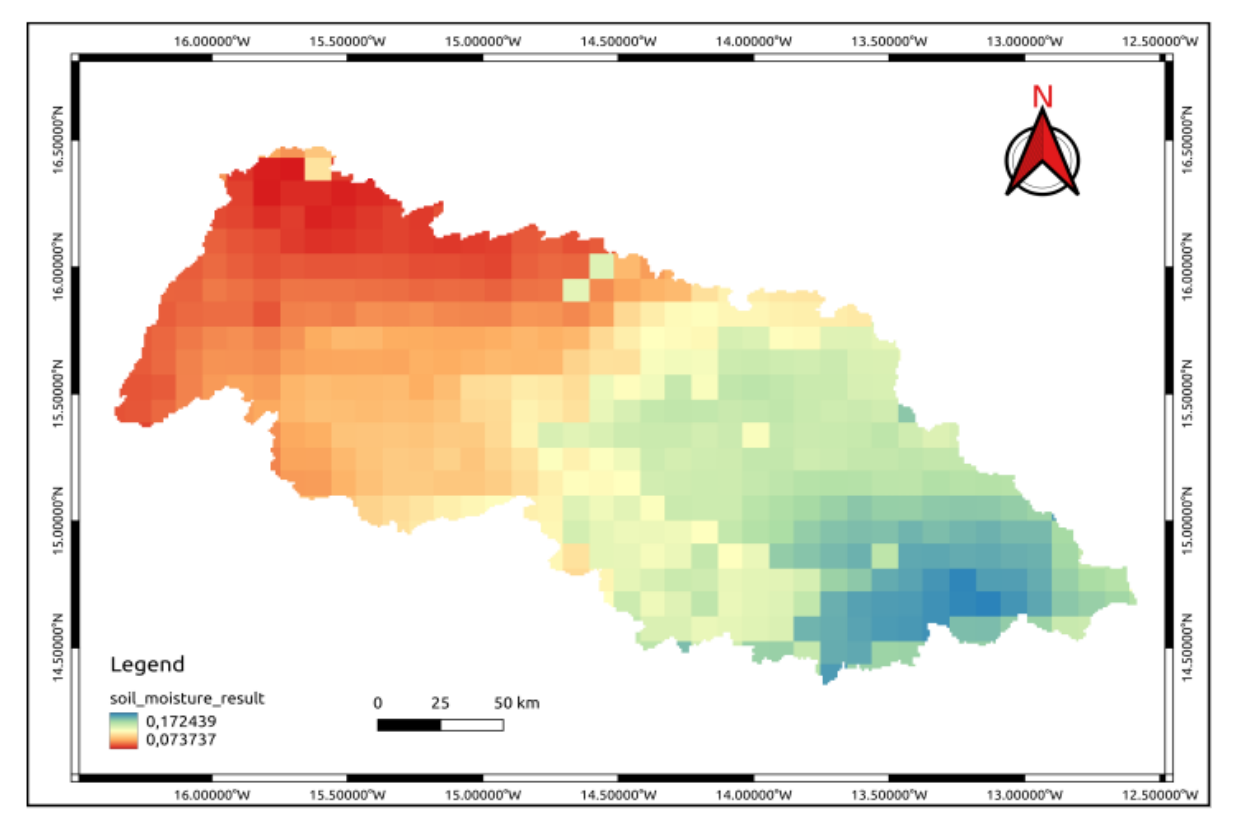


Fig. 8. Average Surface Soil Moisture (0–5 cm) in the Ferlo Area, June–August 2023.

3.2.2 Temporal variation of hydroclimatic indices

In this section, the climate indices are calculated from 1971 to 2100 at reference stations like Richard-toll, Ranerou, Barkedji, and Velingara-ferlo.

3.2.2.1 Temporal variation of rainfall intensity and accumulation

Figure 9 shows the temporal evolution of daily precipitation intensity for four reference stations: Richard-Toll, Barkedji, Ranérou, and Vélingara-Ferlo. Historical data (1971–2005) are represented in black, while future projections under the RCP 4.5 and RCP 8.5 climate scenarios (2006–2100) are shown in blue and red, respectively. The average precipitation intensity generally ranges from 3.5 to 4.3 mm per day, with irregular variations over time and across stations. The northern stations, Richard-Toll and Barkedji, exhibit lower and relatively stable intensities. instance, Richard-Toll shows a historical intensity of around 4 mm/day, with a slight decrease around 2000. Under RCP 4.5, strong variability is observed, with an initial peak followed by a gradual decrease after 2040. Under RCP 8.5, intensity first increases and then stabilizes around 4 mm/day. Barkedji shows a slight decrease before 2000 and relatively stable projecttions between 3.5 and 4 mm/day, with less fluctuation compared to Richard-Toll. The southern stations, Ranérou and Vélingara-Ferlo, exhibit higher intensities and more pronounced variations. Ranérou shows a slight historical decrease before 2000, followed by projections fluctuating around 4 mm/day, with peaks around 2030 and

2080, and a slight downward trend at the end of the period under RCP 8.5. Vélingara-Ferlo begins with historical intensity (~5 mm/day), which significantly decreases around 2000. Future projections indicate an average intensity of around 4 mm/day with regular fluctuations, followed by a notable decrease toward the end of the century, especially under RCP 8.5. Future scenarios show variations around the 1976–2005 mean, sometimes higher and sometimes lower. Notably, between 2041 and 2056, a decrease in intensity is projected at Richard-Toll under both scenarios, while at Ranérou, a similar decline is expected between 2051 and 2085. This figure illustrates significant variability in daily precipitation intensity depending on location and climate scenario. In summary, northern stations show lower and more stable intensities, whereas southern stations exhibit higher intensities with more pronounced fluctuations. The RCP4.5 and RCP8.5 scenarios follow generally similar trajectories, with a more marked downward trend under RCP8.5 by the end of the 21st century. Contrary to the spatial variation of the daily precipitation intensity according to the reference stations, the interannual accumulation is much greater at the southern stations than at the northern stations (Figure 10). In fact, the overall average of the models shows a very irregular interannual variation over time with significant values in the past (1971-2005) but decreasing in the future under the two scenarios RCP4.5 and At RCP8.5. $_{
m the}$ station level, the interannual average cumulative rainfall is around 160 mm at Richard-Toll, 267 mm at the Barkedji, and 281 mm at the Ranérou stations. An average cumulative value of 325 mm is observed over the whole period in the southern zone represented by the Velingara Ferlo station.

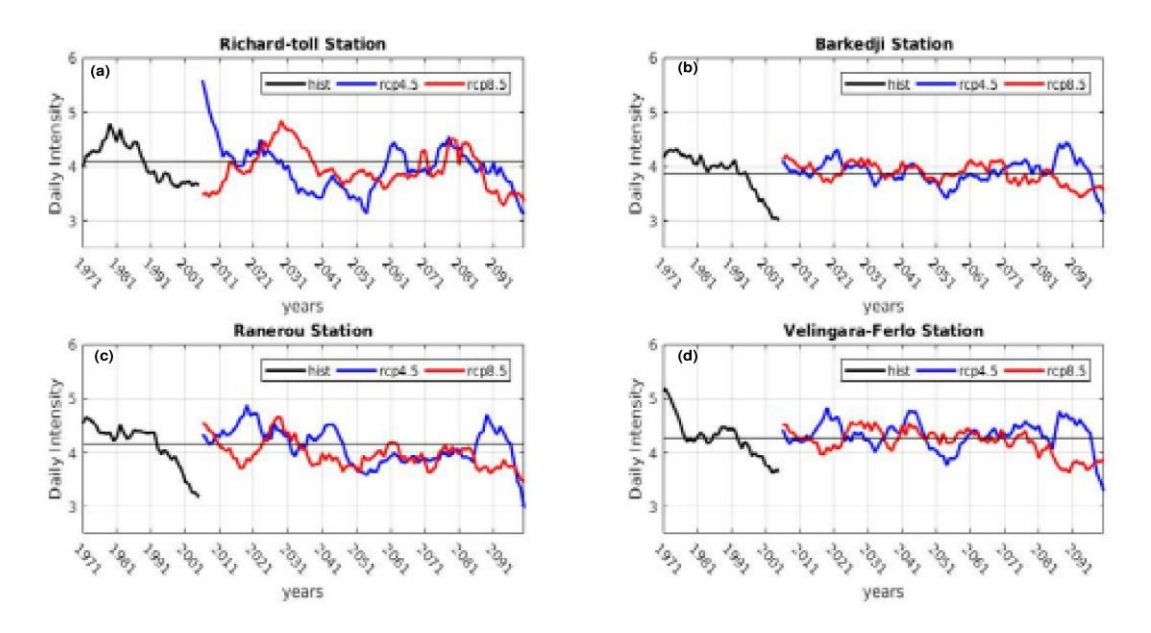


Fig. 9. Time evolution, from 1971 to 2100, of the multi-model mean (MMM), of the seasonal mean of precipitation intensity in Richal-toll (a), Barkedji (b), Ranerou (c), and Velingara Ferlo (d). Black color is for the historical period, Blue color is for RCP4.5, and Red color is for RCP8.5.

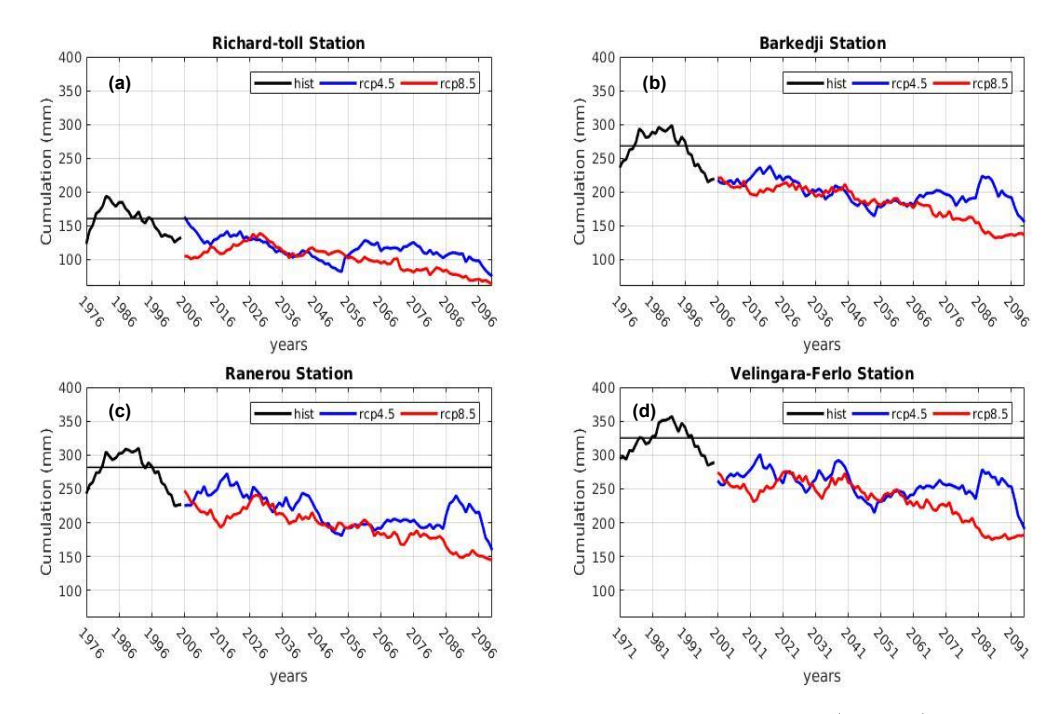


Fig. 10. Time evolution from 1971 to 2100 of the multi-model mean (MMM), of cumulus in Richaltoll(a), Barkedji (b), Ranerou (c) and Velingara Ferlo (d). Black color is for the historical period, Blue color is for RCP4.5 and Red color is for RCP8.5.

3.2.2.2 Spatial variation in the length of the rainy season

Figure 11 gives a characteristic for the three stations (Ranerou, Barkedji, Velingara - Ferlo) during the periods 1971 to 2005 (historical period) and 2006 to 2100 (future) under the scenarios RCP4.5 and RCP8.5.

In Table 2, the ensemble average of the models showed a season length ranging from 89 to 103 days in the period 1971-2005 and varies from 84 to 98 days in the period 2006 to 2100 under the RCP4.5 and RCP8.5 scenarios.

At the Ranérou station, the period of 1971 to 2005 recorded a season of 94 days, but will decrease to 90 and 88 days in the period of 2006 to 2100 under the RCP4.5 and RCP8.5 scenarios, respectively. In Barkedji station, we recorded by the ensemble mean 89 days on the historical part and decreased to 85 and 84 days, respectively, in the future under the RCP4.5 and RCP8.5 scenarios. At Vélingara-Ferlo, we note a season length of 103 days in the past (1971-2005) and will observe a decrease in the future to 98 and 97 days under the scenario.

This variation in length is irregular in time and space (Figure 9), with much higher values in the south than in the north, but also increases more under the RCP48.5 scenario than under the RCP4.5 scenario. The latter results are aligned with those of

[27], who suggests that the average length of the rainy season decreases from south to north in Senegal.

3.2.2.3 Runoff coefficient

The runoff coefficient is often used to assess runoff potential. In the Ferlo watershed, it is calculated to determine the relationship between rainfall and runoff. This coefficient is highly sensitive to the degree of surface waterproofing, as well as to the slope and the connectivity of runoff surfaces.

The results based on this index (Figure 12) calculated from our reference station, which is Richard-toll, show that in the past (1976 to 2005) the runoff coefficient was around 0.35 with the maximum observed in the 2005 year.

In the future, the scenarios show a significant decrease in the runoff coefficient under both RCP4.5 and RCP8.5. This trend, observed across several stations, could be explained by multiple factors. One major factor is the increase in vegetation cover due to changes in rainfall patterns, which promotes greater infiltration and reduces surface runoff. Additionally, soil types with higher permeability may further limit runoff. The geographical location of some stations, such as Richard-Toll, which is situated in a relatively flat area with sandy soils, also contributes to lower runoff coefficients under future climate conditions.

Table 2 Length of the rainy season in the period 1971-2100.

Periods	Historical (1971-2005)	RCP4.5 (2006-20100)	RCP8.5 (2006-2100)
Stations			
Barkedji Station	89 days	85 days	84 days
Ranerou Station	94 days	90 days	88 days
Velingara Station	103 days	98 days	97 days

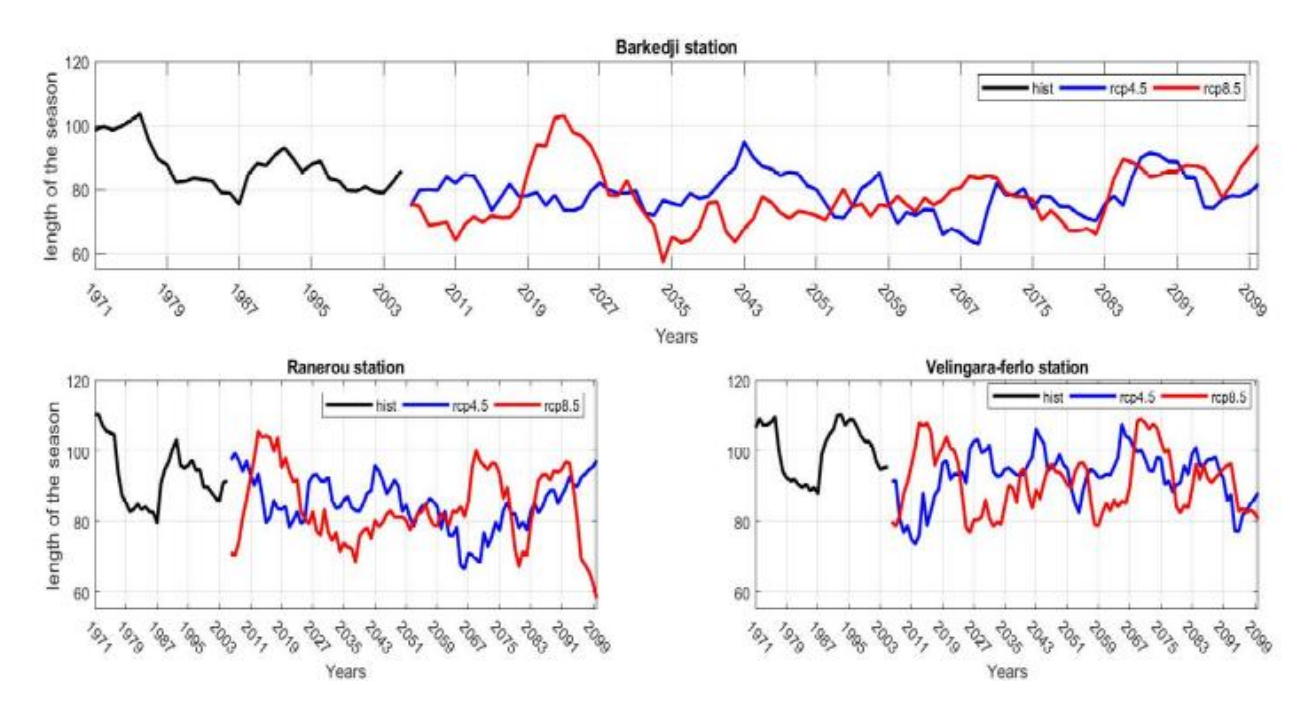


Fig. 11. Time evolution, from 1971 to 2100, of the multi-model mean (MMM), of the length of the season in Barkedji, Ranerou and Velingara Ferlo. Black color is for the historical period, Blue color is for RCP4.5, and Red color is for RCP8.5.

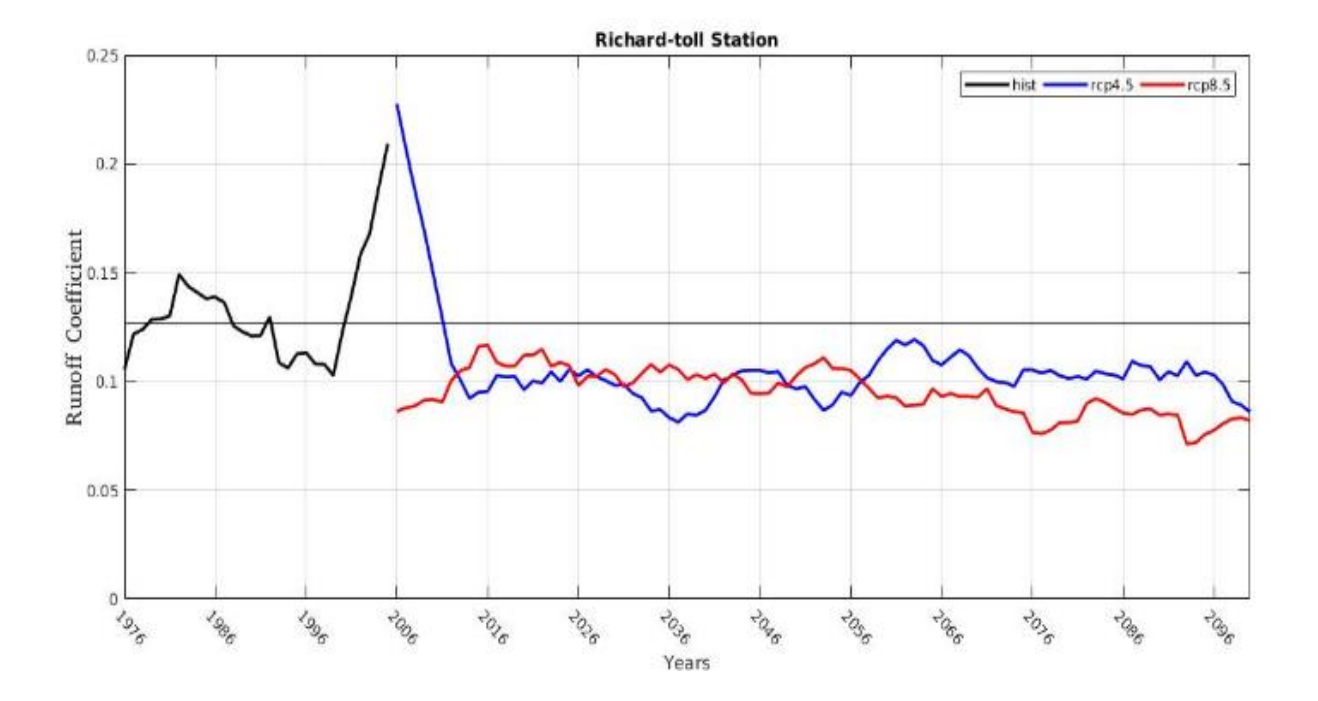


Fig. 12. Runoff coefficient from 1976 to 2100 on the Richard-Toll station calculated from REMO model data. Black color is for the historical period, Blue color is for RCP4.5 and Red color is for RCP8.5.

3.2.2.4 Comparative Analysis of Surface and Base Flow

The term flow always refers to the gravitational circulation of water. It covers several realities depending on the depth at which we are located.

To determine which of these flows predominates in the Ferlo watershed, the proportionality ratio is calculated from the total flow.

The results show an irregular variation in the proportionality ratios throughout the Ferlo area (Figure 13). At the Barkedji Ranérou and Velingara-Ferlo stations, the proportionality ratio of the surface flow is much higher than the proportionality ratio of the base flow during the wettest months (August and September). Contrary to these months, June, July, October, and November are marked by the dominance of base flow over surface flow.

At the Richard-toll station, surface runoff dominates from June to November; this dominance over base flow could be consistent with the results found in the runoff coefficient (Figure 11).

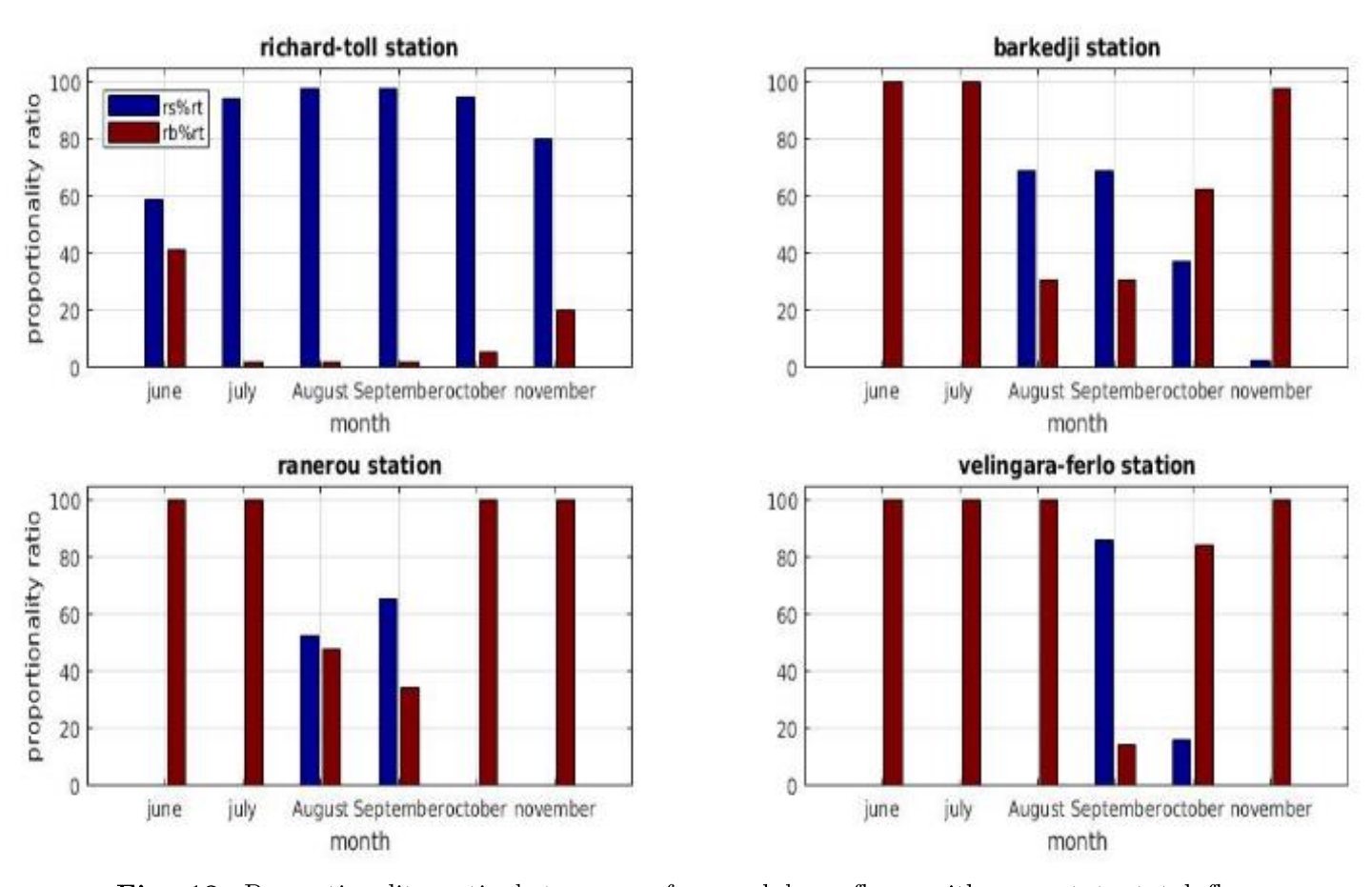


Fig. 13. Proportionality ratio between surface and base flows with respect to total flow (JJASON) from 1976 to 2005 in the Ferlo watershed calculated from the REMO mode.

4 Conclusion

The study projects a future decrease in annual rainfall across the basin, marked by a northward shift of isohyets—specifically, the disappearance of the 600 mm isohyet in the south and the emergence of the 200 mm isohyet in the northern Ferlo. This shift indicates a general regional reduction in rainfall, with the north experiencing a more significant decline than the south. Under the RCP4.5 scenario, rainfall reductions range from 3% to 8%, while under the more severe RCP8.5 scenario (2071–2100), decreases are between 15% and 45%.

precipitation intensity irregular spatial and temporal variability. In the near future (2021–2050), both scenarios predict decreased intensity in the northern and central-eastern basin (up to 8%) but slight increases (2–10%) elsewhere. By 2071–2100, intensity declines almost basin-wide, especially in the north (-8 to -10%) under RCP8.5. Intensity averages 5-10 mm/day, with some stations like Richard-toll recording peaks above 15 mm/day. The rainy season length is expected to decrease by 10–15% in the north and 5% in the south under RCP4.5 in the near term, whereas RCP8.5 forecasts a 5% increase in the southeast. In the distant future, the rainy season shortens uniformly, with up to 25%almost reductions in the northwest. Average rainy season durations slightly decrease across stations under RCP8.5. Runoff coefficients show declines (-10 to -100%) in the south and center but increases (+10 to +120%)in the north initially. Under RCP8.5 in the distant future, northern runoff decreases to +10 to +30%.

Results align with other Senegalese studies but highlight overestimation of rainy season length, possibly affecting onset projections. Future work should improve bias corrections, use more models, and consider alternative agro-climatic methods. Additionally, reforestation efforts like the Great Green Wall since 2006 may influence climate dynamics and model accuracy.

Acknowledgements

The authors thank the Laboratory Oceanography of Sciences and Environment and Climate (LOSEC) of Assane Seck University in Ziguinchor, where the work was done.

References

- [1] A. Kamagaté, Y.B. Koffi, A.M. Kouassi, B.D. Kouakou, D. Seydou, Impact des Évolutions Climatiques sur les Ressources en eau des Petits Bassins en Afrique Sub-Saharienne: Application au Bassin Versant du Bandama à Tortiya (Nord Côte d'Ivoire), Eur. Sci. J. 15(9) (2019) 84-105.
 - doi: 10.19044/esj.2019.v15n9p84
- [2] IPCC, Part A: Global and Sectoral Aspects. (Contribution of Working Group II to the Fifth Assessment Report of the Intergovernmental Panel on Climate Change), Clim. Chang. 2014 Impacts, Adapt. Vulnerability (2014) 1132.

 $\label{lem:https://www.ipcc.ch/pdf/assessment-report/ar5/wg2/WGIIAR5-} FrontMatterA_FINAL.pdf$

[3] B. Sultan, R. Lalou, M. A. Sanni, A. Oumarou, M.A. Soumaré, Les sociétés rurales face aux changements climatiques et environnementaux en

- Afrique de l'Ouest, Synthèses, IRD Éditions, Marseille (2015). https://doi.org/10.4000/books.irdeditions. 8914.
- [4] IPCC, Climate Change, Synthesis Report Summary Chapter for Policymakers (2014) 31.
- [5] S. Ardoin-Bardin et al., Using general circulation model outputs to assess impacts of climate change on runoff for large hydrological catchments in West Africa, Hydrol. Sci. J. 54(1) (2009) 77–89.

doi: 10.1623/hysj.54.1.77

[6] V. Aich et al., Comparing impacts of climate change on streamflow in four large African river basins, Hydrol. Earth Syst. Sci. 18(4) (2014) 1305– 1321.

doi: 10.5194/hess-18-1305-2014

- [7] C. Faye, Examination of water Storage in the Senegal River Basin for a socioeconomic development of downstream river countries, International Journal of Current Science and Engineering 2 (2019) 54-62.
- [8] S. Salack, C. Klein, A. Giannini et al., Global warming induced hybrid rainy seasons in the Sahel, Environ. Res. Lett. 11(10) (2016) 104008. doi: 10.1088/1748-9326/11/10/104008
- [9] République du Sénégal, Contribution prévue déterminée au niveau national (Planned contribution determined at national level) (2015) 1–19.
- [10] T. Ba, L. E. Akpo, A.A. Diouf, Dynamique spatio-temporelle des écosystèmes du bassin versant du Ferlo (Nord-Sénégal) (2017). http://www.m.elewa.org/JAPS;ISSN2071-7024

- [11] G. Faye et al., P.L. Frison, S. Wade, J.A. Ndione, A.C. Beye, J.P. Rudant, Étude de la saisonnalité des mesures des diffusiomètres SCAT: apport au suivi de la végétation au Sahel, cas du Ferlo au Sénégal, Rev. Télédétection 10(1) (2011) 23-31.
- [12] F. Giorgi, C. Jones, G. Asrar, Addressing climate information needs at the regional level: The CORDEX framework, World Meteorol. Org. (WMO) Bull. 58(3) (2009) 175–183.
- [13] M.L. Mbaye, S. Diatta, A.T. Gaye, Climate Change Signals Over Senegal River Basin Using Regional Climate Models of the CORDEX Africa Simulations. In "Lecture Notes of the Institute for Computer Sciences, Social-Informatics and Telecommunications Engineering, LNICST", Springer Verlag (2018) 123–132. doi: 10.1007/978-3-319-98878-8 12
- [14] M.L. Mbaye, S. Hagemann, A. Haensler, T. Stacke, A.T. Gaye, A. Afouda, Assessment of Climate Change Impact on Water Resources in the Upper Senegal Basin (West Africa), Am. J. Clim. Chang. 4(1) (2015) 77–93. doi: 10.4236/ajcc.2015.41008
- [15] E. Gbobaniyi et al., Climatology, annual cycle and interannual variability of precipitation and temperature in CORDEX simulations over West Africa, Int. J. Climatol. 34(7) (2014) 2241–2257. doi: 10.1002/joc.3834
- [16] A. Haensler, F. Saeed, D. Jacob, Assessing the robustness of projected precipitation changes over central Africa on the basis of a multitude of global and regional climate projections, Clim. Chang. 121(2) (2013) 349–363.

doi: 10.1007/s10584-013-0863-8

- [17] G. Nikulin, C. Jones, F. Giorgi et al., Precipitation climatology in an ensemble of CORDEX-Africa regional climate simulations, J. Clim. 25(18) (2012) 6057–6078. doi: 10.1175/JCLI-D-11-00375.1
- [18] M.V.K. Sivakumar, Predicting rainy season potential from the onset of rains in Southern Sahelian and Sudanian climatic zones of West Africa, Agric. For. Meteorol. 42(4) (1988) 295–305. doi: 10.1016/0168-1923(88) 90039-1
- [19] R.H. Moss, J.A. Edmonds, K.A. Hibbard et al., The next generation of scenarios for climate change research and assessment, Nature 463(7282) (2010) 747–756. doi: 10.1038/nature08823
- [20] A. Fall, Ferlo sénégalais: approche géographique de la vulnérabilité des anthroposystèmes sahéliens, Thèse, Université Paris 13, Sorbonne Paris Cité, France (2014). https://hal.science/tel-01622314/document
- [21] M. Tall, M.B. Sylla, I. Diallo et al.,

 Projected impact of climate change in
 the hydroclimatology of Senegal with a
 focus over the Lake of Guiers for the
 twenty-first century, Theor. Appl.
 Climatol. 129(1–2) (2017) 655–665.
 doi: 10.1007/s00704-016-1805-v
- [22] A.B. Sarr, M. Camara, I. Diba, Spatial Distribution of Cordex Regional Climate Models Biases over West

- Africa, Int. J. Geosci. 6(9) (2015) 1018–1031. doi: 10.4236/ijg.2015.69081
- [23] K.E. Kouakou, Z.A. Kouadio, F.W. Kouassi, A. Goula Bi, I. Savane, Modélisation de la température et de la pluviométrie dans un contexte de changement climatique: cas de l'Afrique de l'Ouest, Afrique Sci. 10(1) (2014) 145–160.
- [24] M. Camara, I. Diba, A. Diedhiou, Effects of Land Cover Changes on Compound Extremes over West Africa Using the Regional Climate Model RegCM4, Atmosphere 13(421) (2022)1-17.

doi: 10.3390/atmos13030421

- [25] I. Diallo, F. Giorgi, A. Deme, M. Tall, L. Mariotti, A.T. Gaye, Projected changes of summer monsoon extremes and hydroclimatic regimes over West Africa for the twenty-first century, Clim. Dyn. 47(12) (2016) 3931–3954. doi: 10.1007/s00382-016-3052-4
- [26] D. Faye et al., Regionalization of the Onset and Offset of the Rainy Season in Senegal Using Kohonen Self-Organizing Maps, Atmosphere 15(3) (2024) 1–22. doi: 10.3390/atmos15030378
- [27] J. B. Ndong, Caractérisation De La Saison Des Pluies Dans Le Centre-Ouest Du Sénégal, Publ. l'Association Int. Climatol. 15(1) (2003) 326–332. http://www.climato.be/aic/colloques/actes/PubAIC/art_2003_vol15/Article 40 JB Ndong.pdf